PERGAMON

International Journal of Solids and Structures 37 (2000) 3253–3275

INTERNATIONAL JOURNAL OF SOLIDS and STRUCTURES

www.elsevier.com/locate/ijsolstr

On singularities in composite piezoelectric wedges and junctions

X.-L. Xu, R.K.N.D. Rajapakse*

Department of Civil and Geological Engineering, University of Manitoba, 15 Gillson Street, 342 Engineering Building, Winnipeg, Manitoba, Canada, R3T 5V6

Received 4 December 1998; in revised form 20 April 1999

Abstract

The plane problems of piezoelectric wedges and multi-material wedges/junctions involving piezoelectrics are studied in this paper. The study is focused on the singular behaviour of electroelastic fields at the corner of wedges and junctions. The polarization orientation of the piezoelectric medium may be arbitrary. The problem is formulated by extending Lekhnitskii's complex potential functions. In the homogeneous piezoelectric cases of a half plane and a semi-infinite crack, it is shown that the singularity is invariant with respect to the direction of polarization and explicit solutions are derived for homogeneous boundary condition combinations. In general cases involving multi-material systems, the order of singularity is determined by solving a transcendental characteristic equation derived on the basis of boundary conditions and geometry. The accuracy of the numerical algorithm is verified by comparing with the existing results for pure elastic wedges. Numerical results of homogeneous piezoelectric wedges indicate that electric boundary conditions have a significant effect on the order of singularities. A selected set of practically useful wedges and junctions involving piezoelectrics are studied to examine the influence of wedge angle, polarization orientation, material types, and boundary and interface conditions on the order of singularity of electroelastic fields. © 2000 Elsevier Science Ltd. All rights reserved.

Keywords: Piezoelectric; Singularities; Conductors; Electric field; Stress concentrations; Adaptive structures; Wedges; Cracks; Interfaces

1. Introduction

The study of singular behaviour of stresses in elastic wedges is important to the design of wedges (selection of wedge angles, material combinations, etc.) and in the development of failure criteria for

* Corresponding author. Fax: +1-204-474-7513.
E-mail address: rajapak@cc.umanitoba.ca (R.K.N.D. Rajapakse).

0020-7683/00/$ - see front matter © 2000 Elsevier Science Ltd. All rights reserved.
PII: S0020-7683(99)00143-2

such systems. The knowledge of stress singularity at multi-material junctions/wedges is also essential in the application of linear elastic fracture mechanics to such systems and composites. Due to their intrinsic electroelastic coupling behaviour, piezoelectric materials have wide applications as sensors and actuators in the field of adaptive (smart) structures. In these applications, piezoceramic sensors/actuators are embedded in or bonded to a parent structure. An adaptive structure generally has several composite wedges and material junctions involving piezoelectric materials (Fig. 1). In addition, commonly used piezoceramic stack actuators also involve some of the material junctions shown in Fig. 1. A precise understanding of electroelastic singularities at corners of composite piezoelectric wedges and junctions is valuable to the optimum design and failure analysis of piezoceramic actuators and adaptive structures.

In the case of a piezoelectric material, both stress and electric fields at a sharp corner may be singular. This implies that either local mechanical failure due to stress concentration or dielectric failure due to

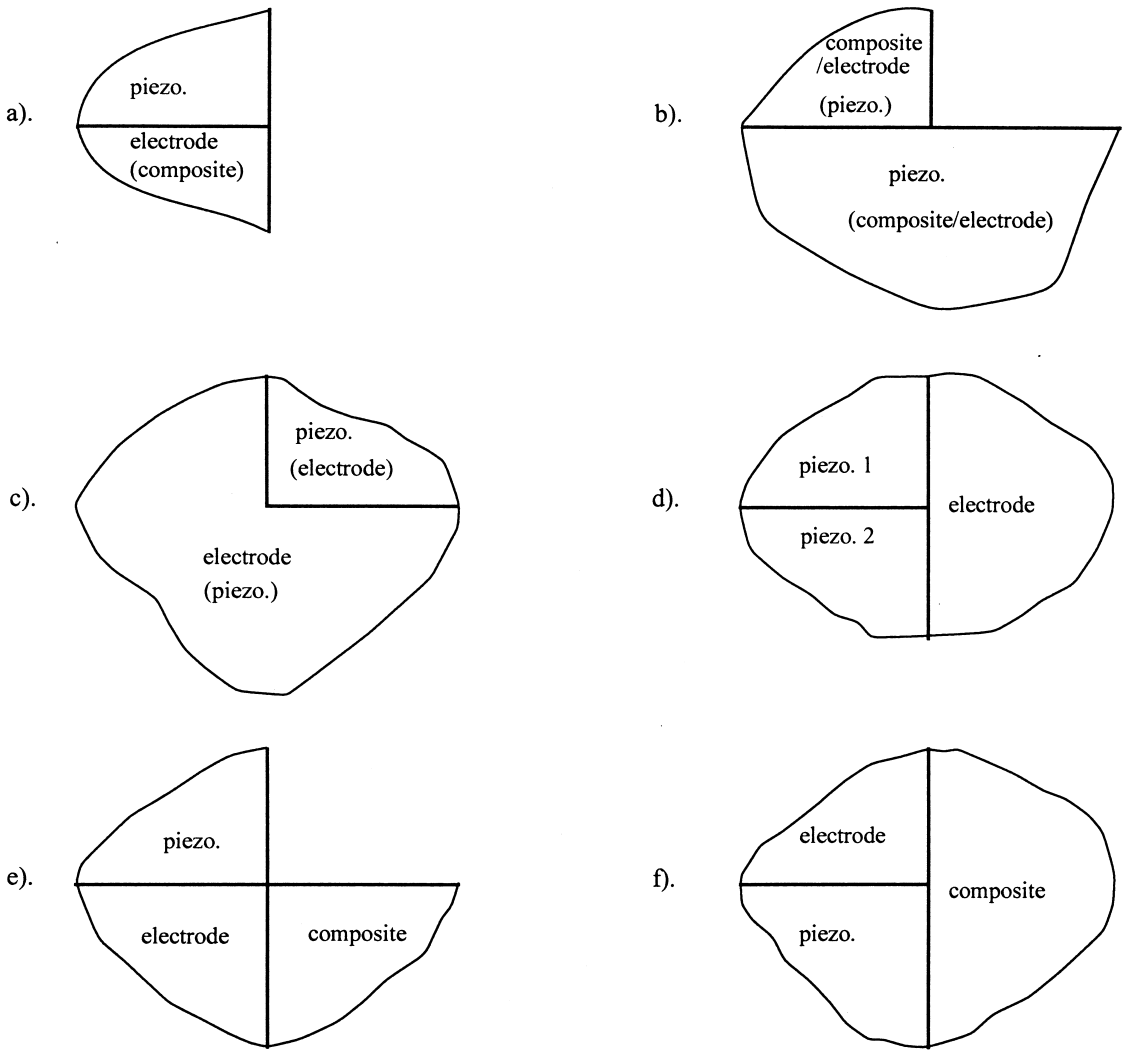

Fig. 1. Composite wedges and junctions encountered in adaptive structures and actuators.

electric field concentration could take place at a sharp corner. A review of literature reveals that a comprehensive analytical and numerical study of electroelastic singularities in composite piezoelectric wedges has not been reported when compared to extensive studies on elastic wedge problems (e.g. Williams, 1952, 1956; Bogy, 1968, 1970; Hein and Erdogan, 1971; Dempsey and Sinclair, 1979; Delale, 1984; Mantič et al., 1997 and others). The only studies that addressed related problems are presented by Sosa and Pak (1990) and Kuo and Barnett (1991). These studies examined electroelastic singularities at the tip of planar cracks perpendicular to the direction of polarization in homogeneous piezoelectrics and bi-material systems.

The main objective of this paper is to examine the electroelastic singularities at the corner of composite piezoelectric wedges/junctions such as those shown in Fig. 1. Lekhnitskii's complex potential functions (Lekhnitskii, 1963) and Williams' eigenfunction expansion (Williams, 1952) are extended to piezoelectric solids. Characteristic equations for different wedges and junctions are established by using boundary conditions and geometry. There is no restriction on the polarization orientation of piezoelectric materials with respect to the wedge/junction geometry in the analysis. Some explicit solutions are obtained for special cases of piezoelectric half planes and cracks. The dependence of electroelastic singularities on wedge angles, material combinations, direction of polarization, and useful interface boundary conditions such as debonded interfaces and cracks is examined for several multi-material systems.

2. Basic equations

Consider a piezoelectric wedge with hexagonal symmetry about or polarized along the direction z' (Fig. 2). Define two Cartesian coordinate systems (x, y, z) and (x', y', z') with $y \equiv y'$ as shown in Fig. 2. The z-axis makes angle β with the direction of polarization z' (β is measured from the z axis in the counter-clockwise direction). The geometry of wedge is defined by the two angles α and φ. A majority of piezoelectric materials used in commercial applications are either hexagonally symmetric crystals or polarized ceramics. The constitutive equations for such materials can be expressed by Eqs. (A1)–(A5) in the Appendix. Assuming planar electroelastic fields independent of y, the constitutive equations with respect to the (x, y, z) system can be expressed as,

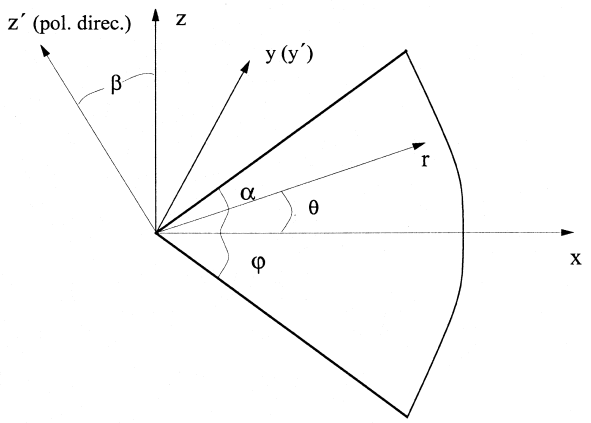

Fig. 2. A piezoelectric wedge.

$$\epsilon_{xx} = a_{11}\sigma_{xx} + a_{12}\sigma_{zz} + a_{13}\sigma_{xz} + b_{11}D_x + b_{21}D_z$$

$$\epsilon_{zz} = a_{12}\sigma_{xx} + a_{22}\sigma_{zz} + a_{23}\sigma_{xz} + b_{12}D_x + b_{22}D_z$$

$$2\epsilon_{xz} = a_{13}\sigma_{xx} + a_{23}\sigma_{zz} + a_{33}\sigma_{xz} + b_{13}D_x + b_{23}D_z$$

$$E_x = -b_{11}\sigma_{xx} - b_{12}\sigma_{zz} - b_{13}\sigma_{xz} + d_{11}D_x + d_{12}D_z$$

$$E_z = -b_{21}\sigma_{xx} - b_{22}\sigma_{zz} - b_{23}\sigma_{xz} + d_{12}D_x + d_{22}D_z \tag{1}$$

where ϵ_{ij}, σ_{ij}, E_i and D_i denote components of strain, stress, electric field and electric displacement, respectively; a_{ij}, b_{ij} and d_{ij} denote elastic, piezoelectric and dielectric constants, respectively. The relationship between electroelastic material properties in the two coordinate systems is given in the Appendix.

Introduce potential functions $F(x, z)$ and $\Phi(x, z)$ as

$$\sigma_{xx} = \frac{\partial^2 F}{\partial z^2}; \quad \sigma_{zz} = \frac{\partial^2 F}{\partial x^2}; \quad \sigma_{xz} = -\frac{\partial^2 F}{\partial x \partial z}; \tag{2}$$

$$D_x = \frac{\partial \Phi}{\partial z}; \quad D_z = -\frac{\partial \Phi}{\partial x}. \tag{3}$$

It can be shown that the equilibrium and Maxwell's equations are automatically satisfied. The above potential function representation can be considered as an extension of Lekhnitskii's representation for elastic solids. Using the strain and electric field compatibility equations for piezoelectric solids, the following sixth-order differential equation can be derived

$$D_1 D_2 D_3 D_4 D_5 D_6 F = 0 \tag{4}$$

where

$$D_n = \frac{\partial}{\partial z} - \mu_n \frac{\partial}{\partial x},$$

and μ_n ($n = 1, \ldots, 6$) are the roots of the characteristic equation

$$l_1(\mu) l_3(\mu) + l_2^2(\mu) = 0 \tag{5}$$

and

$$l_1 = d_{11}\mu^2 - 2d_{12}\mu + d_{22}; \quad l_2 = b_{11}\mu^3 - (b_{21} + b_{13})\mu^2 + (b_{12} + b_{23})\mu - b_{22}$$

$$l_3 = a_{11}\mu^4 - 2a_{13}\mu^3 + (2a_{12} + a_{33})\mu^2 - 2a_{23}\mu + a_{22}.$$

Generally the roots of Eq. (5) are distinct and the solutions of functions F and Φ are of the following form.

$$F(x, z) = \sum_{n=1}^{6} F_n(z_n); \quad \Phi(x, z) = \sum_{n=1}^{6} \delta_n \frac{\partial F_n(z_n)}{\partial z_n} \tag{6}$$

where $z_n = x + \mu_n z$, $\delta_n = l_2(\mu_n)/l_1(\mu_n)$.

The functions $F_n (n = 1, \ldots, 6)$ can be written as power series of z_n. Since this study is focused on singular fields, it is sufficient to consider only the leading term of the power series. Therefore,

$$F(x, z) = \sum_{n=1}^{6} A_n z_n^{\lambda}; \quad \Phi(x, z) = \sum_{n=1}^{6} \lambda \delta_n A_n z_n^{\lambda-1} \tag{7}$$

where λ is the power of the leading term and $A_n (n = 1, \ldots, 6)$ are arbitrary coefficients.

It is convenient to introduce a polar coordinate system (r, θ) as shown in Fig. 2 for the present class of problems. The following solutions for electroelastic fields can be obtained by using Eq. (7) and basic relations in piezoelectricity (Parton and Kudryavtsev 1988).

$$u_r = \lambda \sum_{n=1}^{6} A_n H_{1n} r_n^{\lambda-1}; \quad u_\theta = \lambda \sum_{n=1}^{6} A_n H_{2n} r_n^{\lambda-1}; \quad \phi = \lambda \sum_{n=1}^{6} A_n H_{3n} r_n^{\lambda-1}$$

$$\sigma_{rr} = \lambda(\lambda-1) \sum_{n=1}^{6} A_n H_{7n} r_n^{\lambda-2}; \quad \sigma_{r\theta} = \frac{1}{r}\lambda(\lambda-1) \sum_{n=1}^{6} A_n H_{4n} r_n^{\lambda-1}$$

$$\sigma_{\theta\theta} = \frac{1}{r}\lambda(\lambda-1) \sum_{n=1}^{6} A_n H_{5n} r_n^{\lambda-1}$$

$$D_r = \lambda(\lambda-1) \sum_{n=1}^{6} A_n H_{8n} r_n^{\lambda-2}; \quad D_\theta = \frac{1}{r}\lambda(\lambda-1) \sum_{n=1}^{6} A_n H_{6n} r_n^{\lambda-1}$$

$$E_r = -\frac{1}{r}\lambda(\lambda-1) \sum_{n=1}^{6} A_n H_{3n} r_n^{\lambda-1}; \quad E_\theta = \lambda(\lambda-1) \sum_{n=1}^{6} A_n H_{3n} H_{4n} r_n^{\lambda-2} \tag{8}$$

where u_i denotes the displacement in the i-direction, ϕ denotes the electrical potential, $r_n = r(\cos\theta + \mu_n \sin\theta)$, and

$$H_{1n} = p_n \cos\theta + q_n \sin\theta; \quad H_{2n} = -p_n \sin\theta + q_n \cos\theta; \quad H_{3n} = s_n$$

$$H_{4n} = \sin\theta - \mu_n \cos\theta; \quad H_{5n} = \cos\theta + \mu_n \sin\theta; \quad H_{6n} = -\delta_n$$

$$H_{7n} = (\mu_n \cos\theta - \sin\theta)^2; \quad H_{8n} = \delta_n(\mu_n \cos\theta - \sin\theta)$$

$$p_n = a_{11}\mu_n^2 + a_{12} - a_{13}\mu_n + \delta_n(b_{11}\mu_n - b_{21})$$

$$q_n = (a_{12}\mu_n^2 + a_{22} - a_{23}\mu_n + \delta_n b_{12}\mu_n - \delta_n b_{22})/\mu_n$$

$$s_n = b_{11}\mu_n^2 + b_{12} - b_{13}\mu_n - \delta_n(d_{11}\mu_n - d_{12}).$$

It is worth mentioning that Eq. (8) can also be obtained by utilizing the correspondence between plane piezoelectricity and generalized plane strain in elasticity established recently by Chen and Lai (1997). For example, the equations for the displacements and stresses of an anisotropic elastic wedge developed by Ting (1986) could be used to derive Eq. (8) by following Chen and Lai (1997).

Elastic field and electrical field are decoupled in the case of elastic composites or electrodes, thus the elasticity theory is separated from electrostatics. Polymer based composites are anisotropic and non-conducting materials, therefore, the elastic fields are obtained by setting the coefficients $b_{ij} = d_{ij} = 0$ in Eq. (1). The general solutions for displacements are

$$u_r = \lambda \sum_{n=1}^{4} B_n H'_{1n} r_n'^{\lambda-1}; \quad u_\theta = \lambda \sum_{n=1}^{4} B_n H'_{2n} r_n'^{\lambda-1} \tag{9}$$

where $r'_n = r(\cos\ \theta + \mu'_n\ \sin\theta)$, B_n are arbitrary coefficients, and μ'_n, H'_{1n} and H'_{2n} are defined by Eqs. (A9) and (A10) in the Appendix.

Most conductors used in the adaptive structures are elastic isotropic. The electric field inside an ideal conductor is zero leading to a constant potential (Cheston, 1964). The general solutions for isotropic elasticity for the present class of problems are (Williams, 1952),

$$u_r = \frac{r^{\lambda-1}}{2\mu_0(\lambda-1)}[C_1\ \cos\ \lambda\theta - C_2\ \sin\ \lambda\theta - C_3(\lambda-4k)\cos(2-\lambda)\theta - C_4(\lambda-4k)\sin(2-\lambda)\theta]$$

$$u_\theta = \frac{r^{\lambda-1}}{2\mu_0(\lambda-1)}[-C_1\ \sin\ \lambda\theta - C_2\ \cos\ \lambda\theta + (2-\lambda-4k)(C_3\ \sin(2-\lambda)\theta - C_4\ \cos(2-\lambda)\theta)] \tag{10}$$

where λ_0 and μ_0 are Lame's constants, $k = (\lambda_0 + 2\mu_0)/2(\lambda_0 + \mu_0)$ and $C_n (n = 1, \ldots, 4)$ are arbitrary coefficients.

Examination of the above general solutions for piezoelectrics, anisotropic composites and ideal conductors reveals that singular fields exist only if the real part of λ is less than two. Furthermore, the boundedness of displacement or electric potential at the corner of a wedge requires the real part of λ must be greater than one. Therefore, admissible values of λ are in the range of

$$1 < Re(\lambda) < 2 \tag{11}$$

3. Composite wedges and junctions

In this section, the characteristic equations for composite wedges and junctions are established to determine the admissible values of λ. Consider a piezoelectric wedge as shown in Fig. 2. Possible boundary conditions on two radial edges are traction free ($\sigma_{\theta\theta} = \sigma_{r\theta} = 0$) or clamped ($u_r = u_\theta = 0$) combined with electrically open ($D_i n_i = 0$ or $D_\theta = 0$) or closed ($\phi = 0$ or $E_r = 0$). Electrically open case corresponds to an adjoining medium with zero (or negligible) dielectric constants (e.g. vacuum or air), whereas electrically closed case corresponds to an adjoining ideal conducting medium (Kuo and Barnett, 1991). As shown in Table 1, four basic types of boundary conditions can be considered for a boundary of a piezoelectric medium. The boundary conditions for an elastic medium are traction free ($\sigma_{\theta\theta} = \sigma_{r\theta} = 0$) or clamped ($u_r = u_\theta = 0$). The continuities of the tangential component of the electric field

and the normal component of the electric displacement are demanded at a piezoelectric material interface.

In the remainder of this section, the characteristic equations for composite wedges and junctions are established to determine the admissible values of λ.

3.1. Piezoelectric wedges

There are altogether ten possible combinations of boundary conditions for the two edges of a piezoelectric wedge. For example, traction free and electrically open on both edges (Fig. 2) yield

$$\sigma_{\theta\theta}(\alpha) = \sigma_{r\theta}(\alpha) = D_\theta(\alpha) = 0; \quad \sigma_{\theta\theta}(\varphi) = \sigma_{r\theta}(\varphi) = D_\theta(\varphi) = 0. \tag{12}$$

Using Eqs. (8) and (12) or any other admissible boundary conditions, the following 6×6 homogeneous equation system can be established.

$$[K]\{A\} = \{0\} \tag{13}$$

where $\{A\} = \{A_1, A_2, \ldots, A_6\}^T$ is the vector of unknown coefficients in Eq. (8), $[K]$ is the coefficient matrix whose elements are functions of λ.

A non-trivial solution for Eq. (13) exists if,

$$\det[K(\lambda)] = 0. \tag{14}$$

The determination of admissible values of λ from the above characteristic equation is usually done using a numerical algorithm although analytical solutions can be obtained for a few special cases as shown in a subsequent section.

3.2. Piezoelectrics—conductor/composite wedges and junctions

Referring to Fig. 3, material 1 is assumed to be piezoelectric and material 2 an isotropic elastic ideal conductor. The following continuity conditions can be established at the material interface.

$$u_r^p(0) - u_r^e(0) = 0; \quad u_\theta^p(0) - u_\theta^e(0) = 0; \quad \phi^p(0) = 0$$

$$\sigma_{\theta\theta}^p(0) - \sigma_{\theta\theta}^e(0) = 0; \quad \sigma_{r\theta}^p(0) - \sigma_{r\theta}^e(0) = 0 \tag{15}$$

where subscript p denotes a piezoelectric medium, and e denotes an electric conductor. In addition, a set of admissible boundary conditions on the two outside edges has to be considered (Table 1). For example, the following boundary conditions can be considered on the two outer edges.

Table 1
Admissible basic boundary conditions on edge surfaces

Case	Mechanical	Electric
1	traction free ($\sigma_{\theta\theta} = \sigma_{r\theta} = 0$)	electrically open ($D_\theta = 0$)
2	traction free ($\sigma_{\theta\theta} = \sigma_{r\theta} = 0$)	electrically closed ($\phi = 0$)
3	clamped ($u_r = u_\theta = 0$)	electrically open ($D_\theta = 0$)
4	clamped ($u_r = u_\theta = 0$)	electrically closed ($\phi = 0$)

$$\sigma^{p}_{\theta\theta}(\varphi) = \sigma^{p}_{r\theta}(\varphi) = D^{p}_{\theta}(\varphi) = 0; \quad \sigma^{e}_{\theta\theta}(\alpha) = \sigma^{e}_{r\theta}(\alpha) = 0. \tag{16}$$

Substitution of Eqs. (8) and (10) in Eqs. (15) and (16) results in a homogeneous system of equations similar to Eq. (13) for the ten coefficients $A_n (n = 1, 2, \ldots, 6)$ and $C_n (n = 1, \ldots, 4)$. The admissible values of λ is obtained from the corresponding characteristic equation. In the case of a bi-material junction, Eq. (16) is replaced by a set of interface conditions similar to Eq. (15) corresponding to the other interface.

In the case of piezoelectric/elastic composite wedges and junctions, the condition $\phi^{p} = 0$ is replaced by $D^{p}_{\theta} = 0$ in Eq. (15) to ensure full electric insulation along the bi-material interface.

3.3. Two piezoelectric material wedges

Consider the case of a wedge consisting of two piezoelectric materials as shown in Fig. 3. The two outer edges are assumed to be traction free and electrically insulated. The interface and boundary conditions can be expressed as,

$$u^{p_1}_{r}(0) - u^{p_2}_{r}(0) = 0; \quad u^{p_1}_{\theta}(0) - u^{p_2}_{\theta}(0) = 0; \quad E^{p_1}_{r}(0) - E^{p_2}_{r}(0) = 0;$$

$$\sigma^{p_1}_{\theta\theta}(0) - \sigma^{p_2}_{\theta\theta}(0) = 0; \quad \sigma^{p_1}_{r\theta}(0) - \sigma^{p_2}_{r\theta}(0) = 0; \quad D^{p_1}_{\theta}(0) - D^{p_2}_{\theta}(0) = 0$$

$$\sigma^{p_1}_{\theta\theta}(\varphi) = 0; \quad \sigma^{p_1}_{r\theta}(\varphi) = 0; \quad D^{p_1}_{\theta}(\varphi) = 0$$

$$\sigma^{p_2}_{\theta\theta}(\alpha) = 0; \quad \sigma^{p_2}_{r\theta}(\alpha) = 0; \quad D^{p_2}_{\theta}(\alpha) = 0 \tag{17}$$

where superscript p_1 and p_2 denotes a piezoelectric medium, one and two, respectively.

The substitution of Eq. (8) in Eq. (17) yields a system of homogeneous equations similar to Eq. (13) for the twelve unknown coefficients $A^{p_1}{}_n (n = 1, 2, \ldots, 6)$ and $A^{p_2}{}_n (n = 1, 2, \ldots, 6)$. The admissible values of λ are obtained by solving the corresponding characteristic equation. The above methodology can be directly extended to consider piezoelectric bi-material junctions.

The general procedure to determine the admissible values of λ for multi-material wedges and junctions is identical to the bi-material case except for the presence of more than one interface. The order of the final equation system [Eq. (13)] is determined by the number and type (elastic, piezoelectric) of the

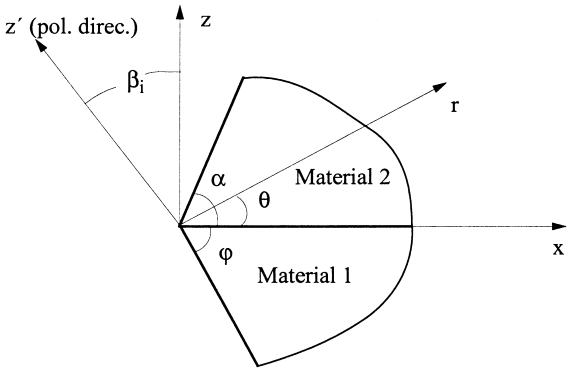

Fig. 3. A bi-material system.

materials. For example, in the case of a three-material wedge with one medium being piezoelectric and the rest elastic materials a 14×14 homogeneous equation system is obtained.

4. Special cases of half plane and crack

The special cases of piezoelectric half planes and semi-infinite cracks are analytically examined in this section.

The geometry of a wedge is defined by two angles α and φ (Fig. 2). A half plane can be defined by (γ, $\gamma \pm \pi$), and a semi-infinite crack by ($\gamma+\pi$, $\gamma-\pi$), where the angle γ can be arbitrary. To study the effect of polarization orientation on the singularities of half planes and cracks, the angle β can be fixed while keeping γ arbitrary. β is set to zero without loss of generality. Eq. (8) can be rewritten in the matrix form as,

$$\mathbf{u}(\theta) = \lambda \sum_{n=1}^{6} A_n \mathbf{h}_1 r_n^{\lambda-1}; \quad \mathbf{t}(\theta) = \frac{1}{r}\lambda(\lambda-1) \sum_{n=1}^{6} A_n \mathbf{h}_2 r_n^{\lambda-1} \tag{18}$$

where $\mathbf{u}(\theta) = \{u_r, u_\theta, \phi\}^T$, $\mathbf{t}(\theta) = \{\sigma_{r\theta}, \sigma_{\theta\theta}, D_\theta\}^T$, $\mathbf{h}_1 = \{H_{1n}, H_{2n}, H_{3n}\}^T$, $\mathbf{h}_2 = \{H_{4n}, H_{5n}, H_{6n}\}^T$.

It can be proven that the characteristic equation for a half-plane or a semi-infinite crack when the boundary of the half-plane or the crack faces are oriented at an angle $\theta = \gamma$ is identical to that at $\theta = 0$. Therefore, for special cases of a piezoelectric half plane and a crack, the singularities are independent of the polarization orientation. This conclusion applies to all admissible boundary condition combinations defined in Table 1.

Consider a piezoelectric half plane $(0, \pi)$ and the direction of polarization β is set to zero without loss of generality. Using Eq. (18) and the boundary condition combinations in Table 1, it is found that combinations 1–1, 2–2, 3–3 and 4–4 all result in the following characteristic equation.

$$\sin \lambda\pi = 0. \tag{19}$$

Apparently, no root of Eq. (19) satisfies the requirement $1 < Re(\lambda) < 2$. Therefore, for piezoelectric half planes, no singularities are found for the homogeneous boundary conditions.

A semi-infinite crack $(\pi, -\pi)$ in a piezoelectric medium with a polarization angle 0° is considered without loss of generality. Consider four homogeneous boundary condition combinations of 1–1, 2–2, 3–3 and 4–4. They all lead to the following characteristic equation.

$$\sin 2\lambda\pi = 0. \tag{20}$$

Only one root, $\lambda = 1.5$, satisfies Eq. (20) resulting in the classical inverse square root type singularity. Kuo and Barnett (1991) employed Stroh's formulation (1962) and obtained the same result for a semi-infinite crack in a piezoelectric medium.

Based on the results by Ting (1986) for general anisotropic elastic wedges, the above conclusions can also be drawn by following the correspondence between plane piezoelectricity and generalized plane strain in elasticity (Chen and Lai, 1997). In the case of free-clamped boundary condition combination for elastic wedges, Ting (1986) showed that, if δ is an order of singularity for a half plane, then $\delta/2$ and $(\delta-1)/2$ are orders of singularities for a semi-infinite crack. It can be easily shown that this conclusion is also applied to any admissible boundary condition combinations for piezoelectric half planes and semi-infinite cracks.

5. Numerical results and discussion

Two polarized piezoceramics, namely PZT-4 and PZT-5 (Berlincourt et al., 1964), graphite/epoxy composite, and two isotropic conductors, aluminum and nickel, are used in the numerical study. The relevant material properties are given below.

PZT-4 (Eqs. (A1) and (A2)):

$$s'_{11} = 10.9 \times 10^{-12}\ \mathrm{m^2/N}, \quad s'_{33} = 7.90 \times 10^{-12}\ \mathrm{m^2/N}, \quad s'_{12} = -5.42 \times 10^{-12}\ \mathrm{m^2/N}$$

$$s'_{13} = -2.10 \times 10^{-12}\ \mathrm{m^2/N}, \quad s'_{44} = 19.3 \times 10^{-12}\ \mathrm{m^2/N}$$

$$g'_{31} = -11.1 \times 10^{-3}\ \mathrm{Vm/N}, \quad g'_{33} = 26.1 \times 10^{-3}\ \mathrm{Vm/N}, \quad g'_{15} = 39.4 \times 10^{-3}\ \mathrm{Vm/N}$$

$$\beta'_{11} = 7.66 \times 10^{7}\ \mathrm{V^2/N}, \quad \beta'_{33} = 8.69 \times 10^{7}\ \mathrm{V^2/N}$$

PZT-5 (Eqs. (A1) and (A2)):

$$s'_{11} = 14.4 \times 10^{-12}\ \mathrm{m^2/N}, \quad s'_{33} = 9.46 \times 10^{-12}\ \mathrm{m^2/N}, \quad s'_{12} = -7.71 \times 10^{-12}\ \mathrm{m^2/N}$$

$$s'_{13} = -2.98 \times 10^{-12}\ \mathrm{m^2/N}, \quad s'_{44} = 25.2 \times 10^{-12}\ \mathrm{m^2/N}$$

$$g'_{31} = -11.4 \times 10^{-3}\ \mathrm{Vm/N}, \quad g'_{33} = 24.8 \times 10^{-3}\ \mathrm{Vm/N}, \quad g'_{15} = 38.2 \times 10^{-3}\ \mathrm{Vm/N}$$

$$\beta'_{11} = 6.53 \times 10^{7}\ \mathrm{V^2/N}, \quad \beta'_{33} = 6.65 \times 10^{7}\ \mathrm{V^2/N}$$

Aluminum (Young's modulus E and Poisson's ratio ν): $E = 68.9$ GPa, $\nu = 0.25$
Nickel: $E = 210$ GPa, $\nu = 0.31$
Graphite/epoxy composite (G is the shear modulus):

$$E_{xx} = 132.8\ \mathrm{GPa}, \quad E_{zz} = 10.76\ \mathrm{GPa}, \quad E_{yy} = 10.96\ \mathrm{GPa}$$

$$G_{zy} = 3.61\ \mathrm{GPa}, \quad G_{xy} = 5.65\ \mathrm{GPa}, \quad G_{xz} = 5.65\ \mathrm{GPa}$$

$$v_{xz} = 0.24, \quad v_{xy} = 0.24, \quad v_{zy} = 0.49$$

The characteristic equation for a wedge/junction is transcendental and has infinite number of roots. The root λ can be real or a complex quantity. Numerical experiments show that the roots are generally complex for composite systems and real roots exist for some cases of piezoelectric wedges. The order of electroelastic singularity is governed by the real part of $(\lambda-2)$. The root of primary interest is the one with the smallest positive real part between one and two. The existence of a non-vanishing imaginary part of $(\lambda-2)$ leads to oscillatory singularity (Suo, 1990). All roots meeting the requirement in Eq. (11) are presented in the numerical study in order to present a complete picture of the nature of singularities in composite piezoelectric wedges/junctions. Plain strain conditions are assumed throughout the computations. A numerical procedure based on Müller's method (Müller, 1956) is used to search for admissible values of λ.

To verify the accuracy of the numerical procedure, the solutions for piezoelectric bi-material wedges are compared with those for isotropic bi-material wedges given by Hein and Erdogan (1971) through a limiting process. Referring to Fig. 3, consider Material 1 and Material 2 as isotropic ideal elastic materials with Young's moduli $E_1/E_2 = 10/31$ and Poisson's ratios $v_1 = 0.22$, $v_2 = 0.30$. Hein and Erdogan (1971) presented the solutions for two wedges, i.e. $\alpha = -\varphi = 90^\circ$ and $\alpha = 90^\circ$, $\varphi = -180^\circ$. To simulate the above isotropic elastic bi-material wedges, set $s'_{11} = 3.23 \times 10^{-1}$ m^2/N, $s'_{33} = 3.23 \times 10^{-1}$ m^2/N, $s'_{12} = -0.97 \times 10^{-1}$ m^2/N, $s'_{13} = -0.97 \times 10^{-1}$ m^2/N, $s'_{44} = 8.39 \times 10^{-1}$ m^2/N as elastic constants of Material 1; $s'_{11} = 10 \times 10^{-1}$ m^2/N, $s'_{33} = 10 \times 10^{-1}$ m^2/N, $s'_{12} = -2.2 \times 10^{-1}$ m^2/N, $s'_{13} = -2.2 \times 10^{-1}$ m^2/N, $s'_{44} = 24.4 \times 10^{-1}$ m^2/N as elastic constants of Material 2. The piezoelectric constants g'_{ij} of the two materials are set to negligible values ($g'_{ij} \to 0$) in order to simulate ideal elastic behaviour. The solutions are compared in Table 3 and very good agreement is observed.

5.1. Piezoelectric wedges

Consider a PZT-4 wedge with polarization direction along the z-axis ($\beta = 0$ in Fig. 2). Without loss of generality, set $\varphi = -\alpha$ in the numerical study. Figs. 4(a) and (b) show the variation of the order of singularity with the wedge angle 2α for the homogeneous boundary condition combinations 1–1 and 4–4 in Table 1, respectively. It is found that all roots are real. The two cases considered have singularities only for reentrant wedges, i.e. wedge angles between 180° and 360°. Two roots exist for all wedge angles between 180° and 360° while a third root appears between 270° and 360°, and 180° and 360° for boundary condition combinations 1–1 and 4–4 respectively. An increase in the order of singularity is noted with increasing wedge angle. For the limiting case of a semi-infinite crack, two of the roots approach the classical value of −0.5. An investigation of wedges with mixed boundary conditions in Table 1 (e.g. 1–4) shows roots for wedge angles less than 180°, and the presence of more than three roots. According to the study of elastic wedges by Mantič et al. (1997), there are in general two roots for traction free B.C. on both edge surfaces, while the present study shows combinations 1–1, 2–2 and 1–2 have three roots. Therefore, piezoelectric wedges generally have one or more extra admissible roots compared to the corresponding elastic case.

Three special cases of wedges, namely a right angle ($2\alpha = 90^\circ$), a half plane ($2\alpha = 180^\circ$) and a semi-infinite crack ($2\alpha = 360^\circ$) are of interest in engineering. Eq. (14) is numerically unstable for $2\alpha = 360^\circ$, and $2\alpha = 359.99^\circ$ was used in the computations. Table 2 shows the order of singularities ($\lambda - 2$) corresponding to the ten possible boundary condition combinations based on Table 1. Numerical results agree with the analytical solution presented earlier for boundary condition combinations 1–1, 2–2, 3–3 and 4–4 for a half plane and a crack. The roots for half planes and cracks in Table 2 are valid for all possible polarization angles β in view of the earlier finding that roots are invariant with β. Table 2 also shows roots for mixed boundary conditions, such as those considered by Kuo and Barnett (1991), on the two edge surfaces. The order of singularity for semi-infinite cracks is stronger than the classical inverse square root singularity and oscillatory type singularities exist for mixed boundary conditions. In addition, up to six admissible roots may exist for some mixed boundary conditions. At least one of the singularities is of inverse square root type for half planes with mixed boundary conditions and oscillatory singularities exist for some cases. Note that the relation between columns 3 and 4 confirms the conclusion given earlier, i.e., if δ is an order of singularity for a piezoelectric half plane, then $\delta/2$ and $(\delta - 1)/2$ are orders of singularities for a semi-infinite crack with identical boundary conditions. The comparison of results between boundary condition combinations in Table 2 indicates that electrical boundary conditions have a significant influence on the order of singularities. In the case of a right angle wedge, singularities exist only for mixed boundary conditions. One admissible root was found and the singularity is normally weaker than that corresponding to a half plane or a crack. No oscillatory type singularities are found.

Figs. 5 and 6 show the effect of polarization orientation (β) on the order of singularities for PZT-4 wedges. In Fig. 5, the dependence of the order of singularity on β is examined for two wedge angles 240°, 300° under traction free and electrically open boundary conditions on both edges. Note under the assumed boundary conditions, singularities exist only for wedge angles greater than 180°. The singularities are identical for orientations β and $-\beta$ showing symmetry about $\beta=0$. The singularity corresponding to $\beta=\pm 90°$ is slightly stronger than that corresponding to $\beta=0$ indicating a weak dependence on the polarization orientation. Oscillatory type singularities are not found. The results for right angle wedges ($2\alpha=90°$) with traction free boundary conditions on one edge surface, i.e.

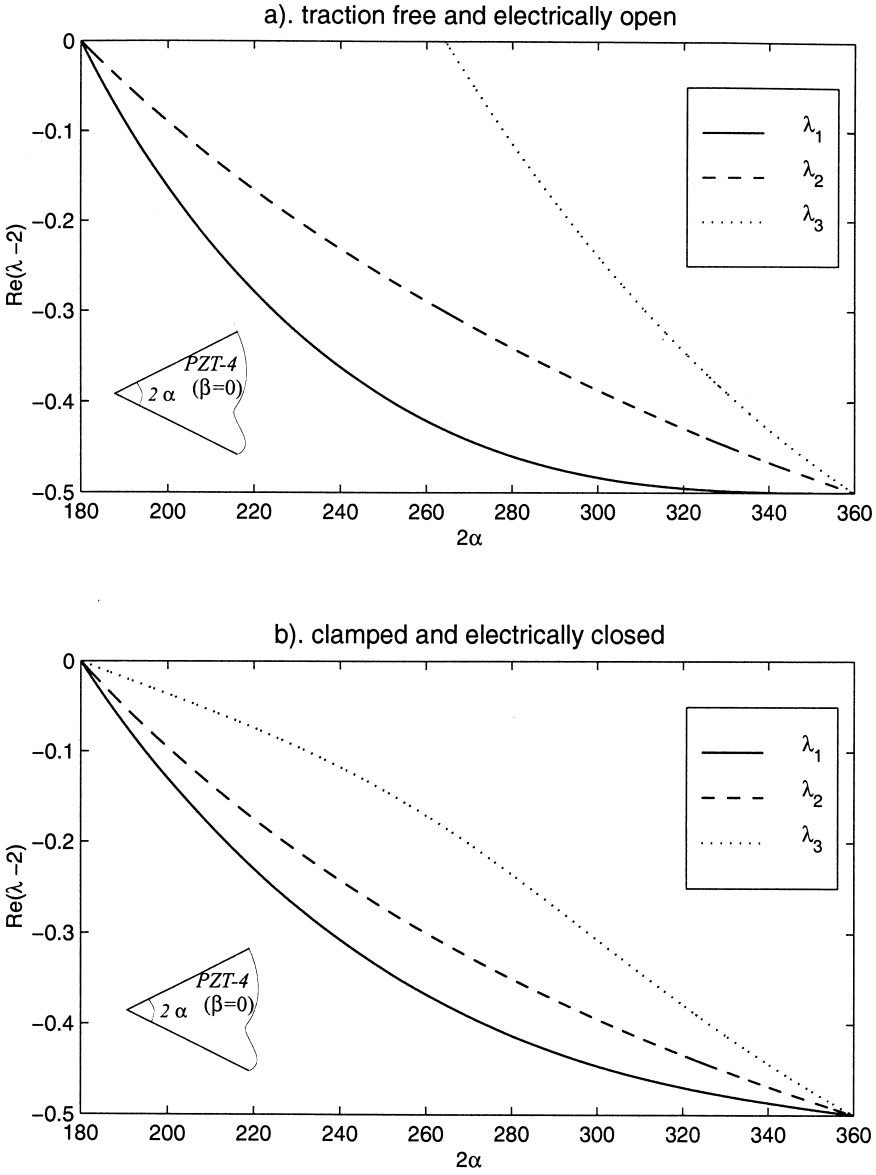

Fig. 4. Variation of the order of singularity with the wedge angle.

Table 2
Order of singularities for a right angle wedge, half plane and crack ($\beta = 0$)

B.C. combinations	Special wedges		
	Right angle	Half plane	Crack
1–1 (2–2, 3–3, 4–4)	–	–	−0.5000
1–2	−0.0731	−0.5000	−0.7500, −0.5000
			−0.2500
1–3	−0.2176	-0.5000 ± 0.14395i	−0.5000
			-0.7500 ± 0.07197i
			-0.2500 ± 0.07197i
1–4	−0.4855	−0.6261	−0.8131, −0.6869
		−0.5000	−0.3131, −0.2500
		−0.3739	−0.1869, −0.7500
2–3	−0.3445	−0.5000	−0.7500, −0.2500
		-0.5000 ± 0.22991i	-0.7500 ± 0.11495i
			-0.2500 ± 0.11495i
2–4	−0.3442	-0.5000 ± 0.04309i	−0.5000
			-0.7500 ± 0.02154i
			-0.2500 ± 0.02154i
3–4	−0.0416	−0.5000	−0.7500, −0.5000
			−0.2500

combinations 1–3, 1–4, 2–3 and 2–4 in Table 1, are shown in Fig. 6. Oscillatory type singularities exist only in the case of combination 2–3. A strong dependence on the polarization orientation is observed for all boundary condition combinations except for 2–4 and the roots are symmetrical about $\beta = 0^\circ$. The combination 1–4 shows two roots for $|\beta| > 45^\circ$ and the strongest or weakest singularity exists when the poling direction is along the z- or x-axis. An exception occurs for the combination 2–3 resulting in the weakest singularity for $\beta \simeq \pm 50^\circ$.

Table 3
Comparison of roots λ for isotropic bi-material wedges (Fig. 3)

Geometry	Present	Hein and Erdogan (1971)
$\alpha = 90^\circ$	1.9494	1.949
$\varphi = -90^\circ$	2.8402 ± 0.2801i	2.840 ± 0.280i
	3.8056 ± 0.8125i	3.800 ± 0.800i
	4.8462 ± 0.8687i	4.850 ± 0.850i
	5.8450 ± 1.1679i	5.900 ± 1.150i
$\alpha = 90^\circ$	1.6474	1.650
$\varphi = -180^\circ$	1.9751	1.977
	2.7332 ± 0.2857i	2.733 ± 0.286i
	3.0780 ± 0.2225i	3.080 ± 0.220i
	3.9988 ± 0.1296i	4.000 ± 0.130i
	4.8453 ± 0.8707i	4.850 ± 0.950i
	5.0015 ± 0.1598i	5.000 ± 0.130i
	5.9997 ± 0.1384i	6.000 ± 0.130i
	1.6388, 2.3526	
	3.6474, 4.3526	
	5.6474	

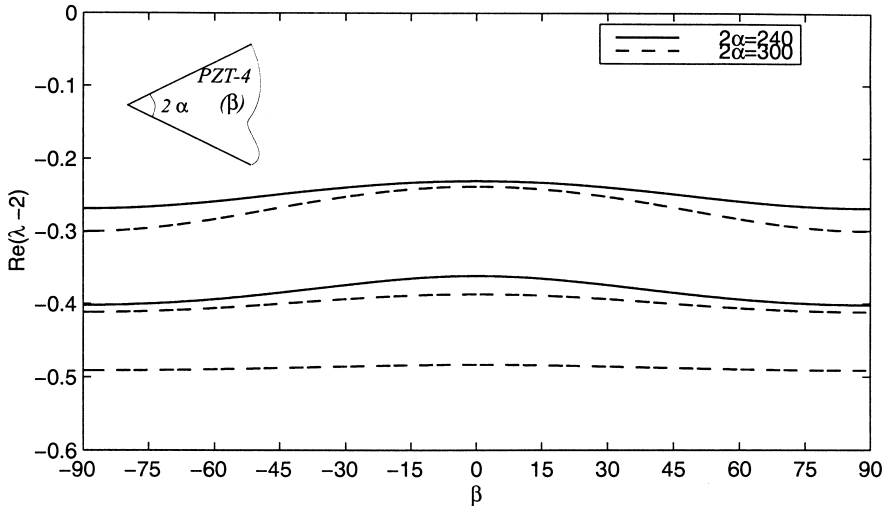

Fig. 5. Variation of the order of singularity with the polarization angle for traction free and electrically open wedges.

A study of PZT-5 wedges show that singularities follow trends similar to those in Figs. 4–6 and Table 2, and the magnitude of roots are also nearly identical.

5.2. Piezoelectric—conductor wedges and junctions

The results for PZT-4–aluminum/nickel wedges and junctions are presented in Figs. 7 and 8. The first case considered (Fig. 7(a)) involves aluminum or nickel (treated as an ideal conductor) quarter plane bonded to a PZT-4 quarter plane. The edges of the PZT quarter planes are traction free and electrically open, and traction free for conductors. Interface conditions are given by Eq. (15). The polarization

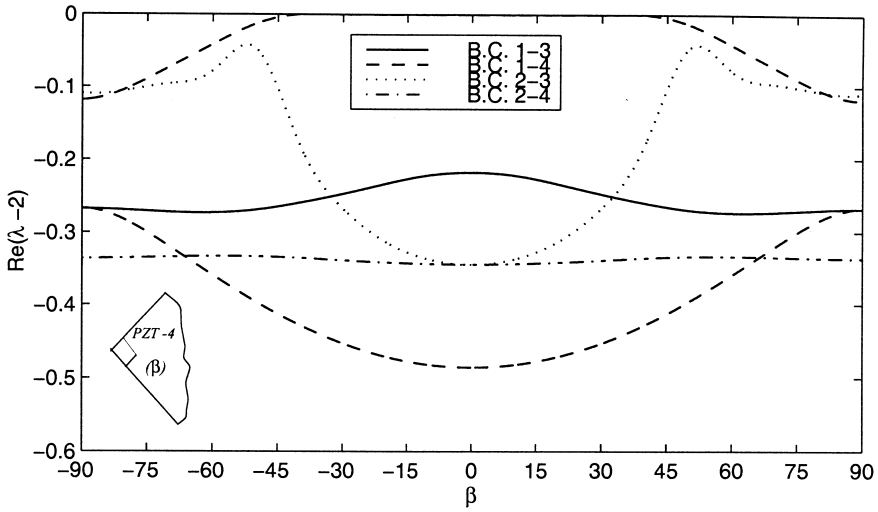

Fig. 6. Variation of the order of singularity with the polarization angle for right angle wedges.

orientation β is varied from 180° to −180°. Only one root is observed for aluminum and two for nickel. The singularity in nickel–PZT wedge is stronger than that in aluminum–PZT wedge. The latter system has a very weak singularity with less dependence on β. The influence of poling direction is more significant in the case of nickel–PZT wedges with $\beta = -45°$, 135° showing the strongest singularities. In general, the singularity is weaker than the classical inverse square root singularity. An aluminum or nickel wedge bonded to a PZT-4 half plane is considered in Fig. 7(b). Setting polarization orientation angle $\beta = 0$, the effect of wedge angle α is investigated. Three roots exist for both nickel and aluminium, and the singularities become more severe as the wedge angle α increases. The case of an interface crack

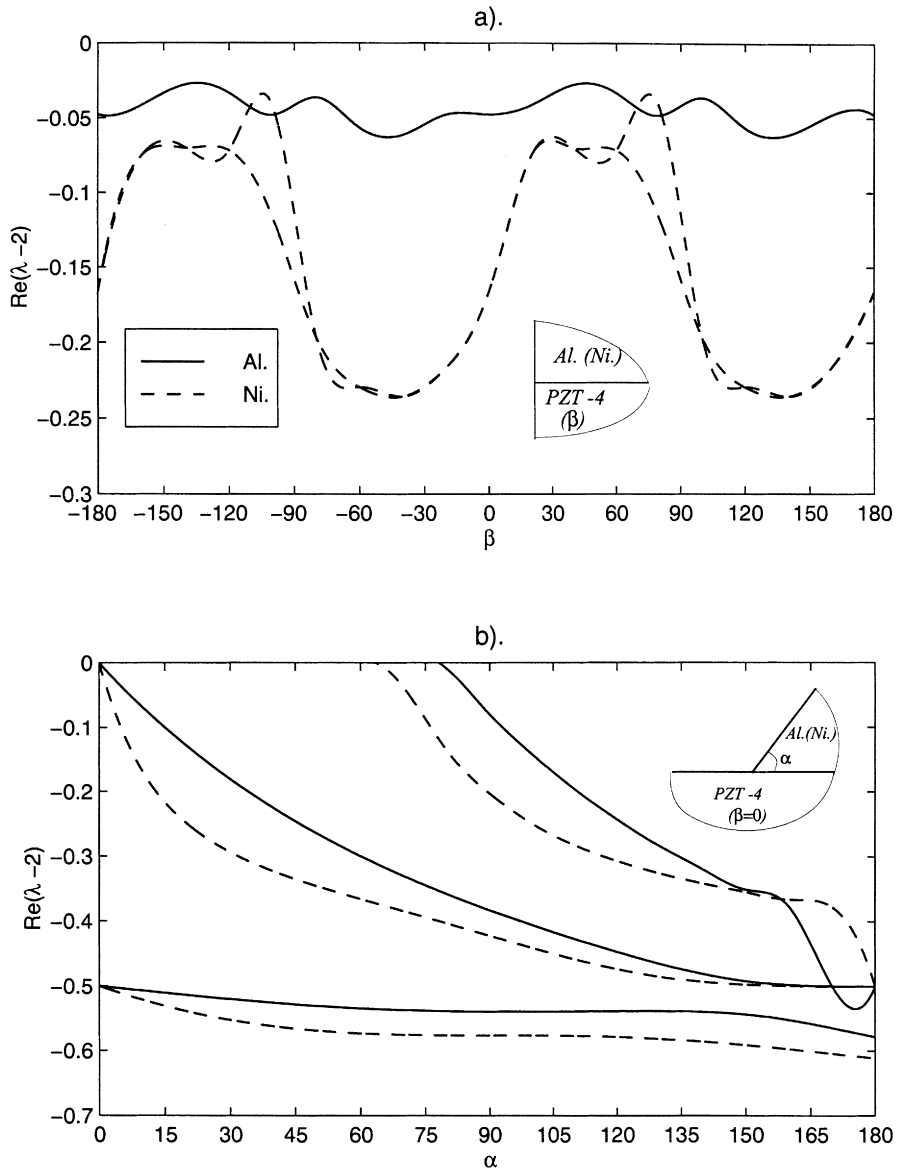

Fig. 7. Order of singularity for PZT-4—aluminium (nickel) wedges.

is obtained when $\alpha = 180^\circ$ and the singularity is found to be stronger than the classical inverse square root singularity for both bi-material systems.

A fully bonded PZT-4–aluminum or nickel junction is considered in Fig. 8(a) for varying angle α and three poling directions ($\beta = 0^\circ$, 90°, 180°). The results for $\beta = 0^\circ$ are identical to that for $\beta = 180^\circ$. No singularity exists when α is less than 180° for both aluminum and nickel. When α is larger than 180°, a very weak singularity is noted for aluminum–PZT system only for $\beta = 90^\circ$. The root corresponding to nickel–PZT system increases rapidly until α is closer to 240° for the three poling directions. An additional root for this system exists for α closer to 270° when $\beta = 90^\circ$. The singularities are weaker than

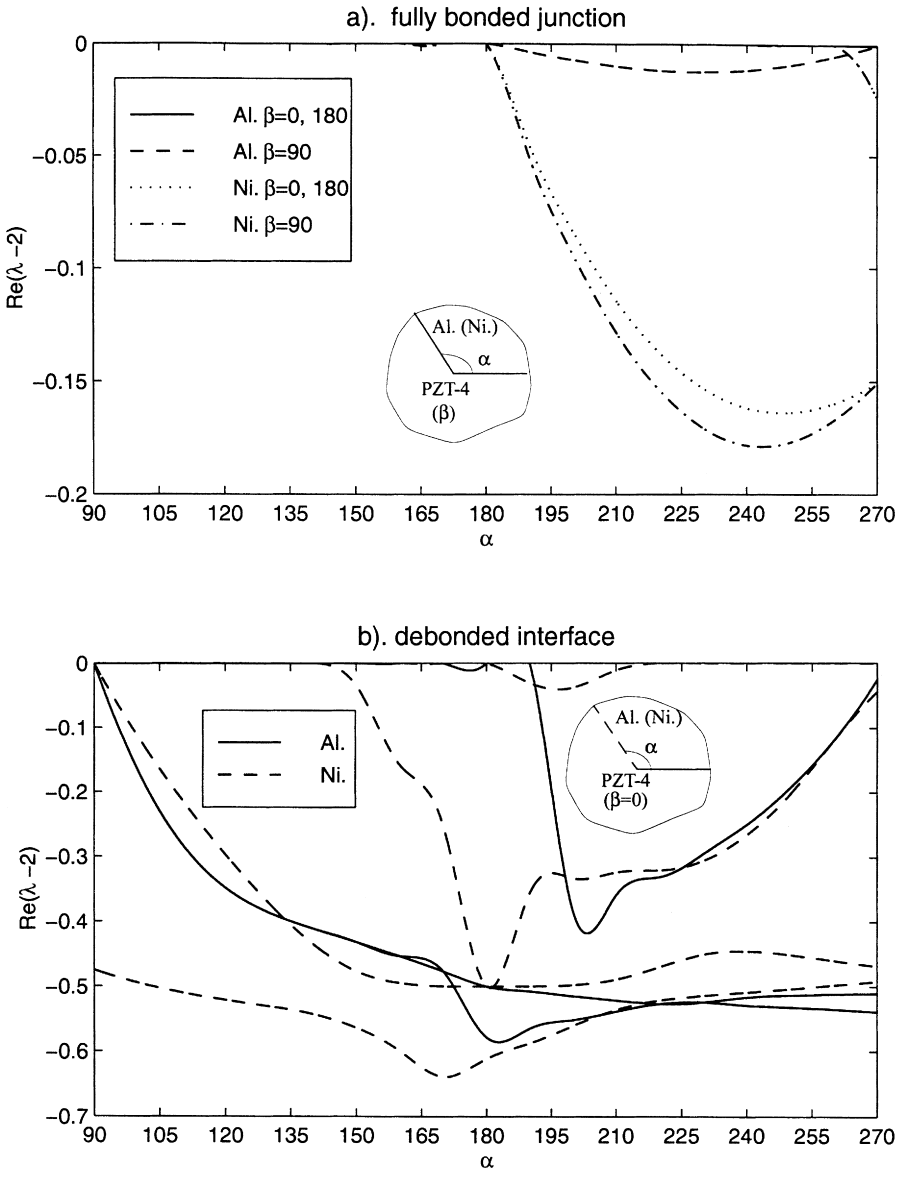

Fig. 8. Order of singularity for PZT-4—aluminium (nickel) junctions.

the classical inverse square root singularity. Consider the same bi-material systems except that the interface defined by angle α is fully debonded and electrically open, as shown in Fig. 8(b). Three roots are found for aluminum, and four for nickel. Singularities exists for all values of α considered and are stronger for both nickel–PZT and aluminum–PZT systems when compared to the fully bonded case in Fig. 8(a). The singularity is also stronger than the classical inverse square root singularity for most α in the case of nickel. Based on the results shown in Figs. 7 and 8, it can be concluded that aluminium-PZT systems have weaker singularities in most cases when compared to nickel-PZT systems. The same

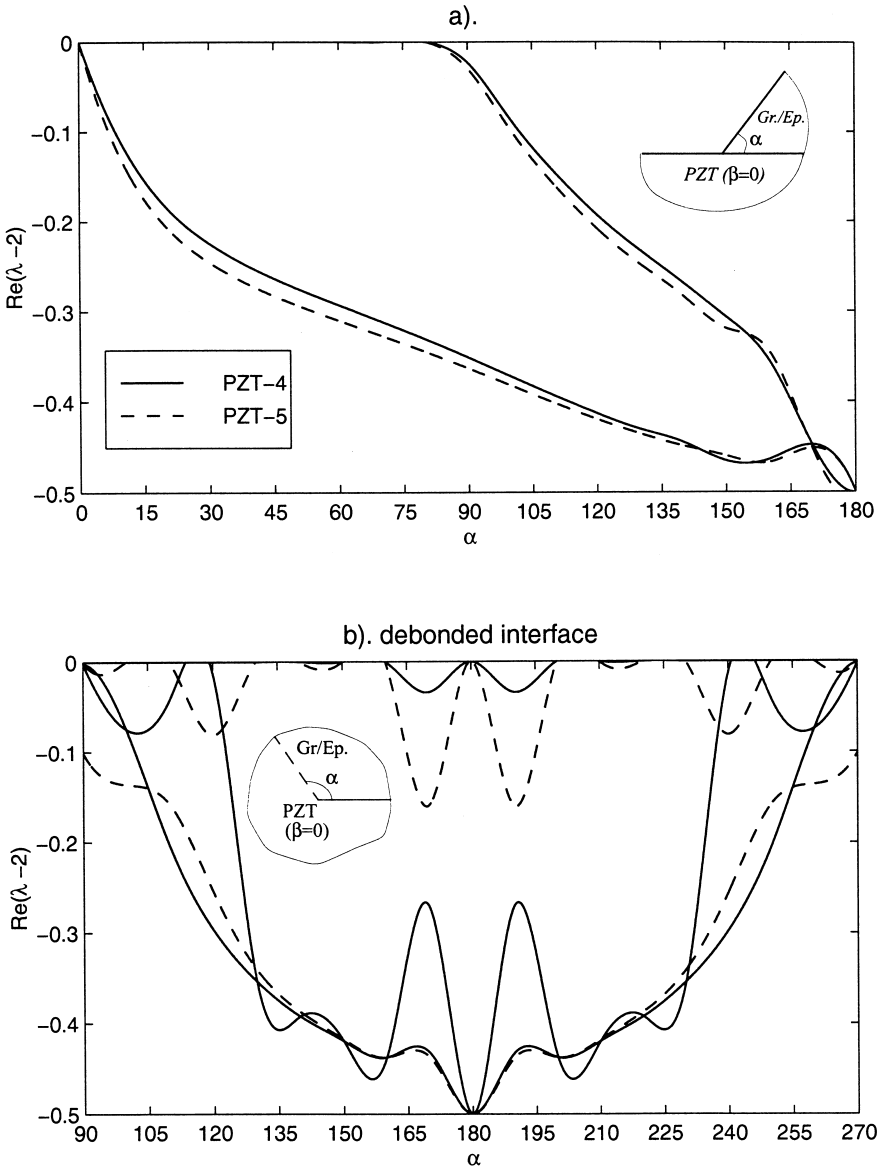

Fig. 9. Order of singularity for PZT—graphite/epoxy systems.

systems are considered with electrically closed boundary conditions on the debonded interface and the results are found to follow trends quite similar to Fig. 8(b) with some difference in the magnitude.

5.3. Piezoelectric—graphite/epoxy wedges and junctions

The roots of a PZT–Gr./Ep. wedge with traction free and electrically open outer edges are shown in Fig. 9(a). The interface is fully bonded and electrically insulated. The influence of wedge angle α on the order of singularity is investigated, while the polarization β is set to zero. Generally two roots exist with one over the full range of α, while another exists only for α larger than 80°. The singularities become stronger as the wedge angle α increases for both PZT-4 and PZT-5. The roots show negligible dependence on the type of piezoelectric material. The case of an interface crack between PZT and Gr./Ep. is obtained when $\alpha = 180°$, and the singularity is identical to the classical inverse square root singularity. A piezoelectric-graphite/epoxy wedge similar to that shown in Fig. 7(a) is also considered and the singularities are found very weak (weaker than -0.06) for the range of β shown in Fig. 7(a).

A completely bonded PZT–Gr./Ep. composite junction similar to that shown in Fig. 8(a) is examined in the numerical study, no singularities are found for the considered range of α. A PZT–Gr/Ep. bi-material junction with a fully debonded and electrically insulated interface is examined in Fig. 9(b). The polarization of PZT is set to 0° with the debonded interface varied from 90° to 270°. Two roots exist for PZT-5 and three for PZT-4. The roots are symmetrical about $\alpha = 180°$ and show strong dependence on α. When α is 180° (interface crack), the classical inverse square root type singularity is observed for both piezoelectric materials. The nonexistence of singularities for a fully bonded bi-material junction and the presence of strong singularities for a debonded junction indicate the importance of interface conditions on the stress field near a sharp corner.

5.4. Piezoelectric bi-material systems

Bi-material junctions involving PZT-4 and PZT-5 with a debonded interface defined by angle α are considered in Fig. 10. Traction free and electrically open boundary conditions are assumed along the debonded interface and full continuity (mechanical and electrical) conditions are assumed on the other

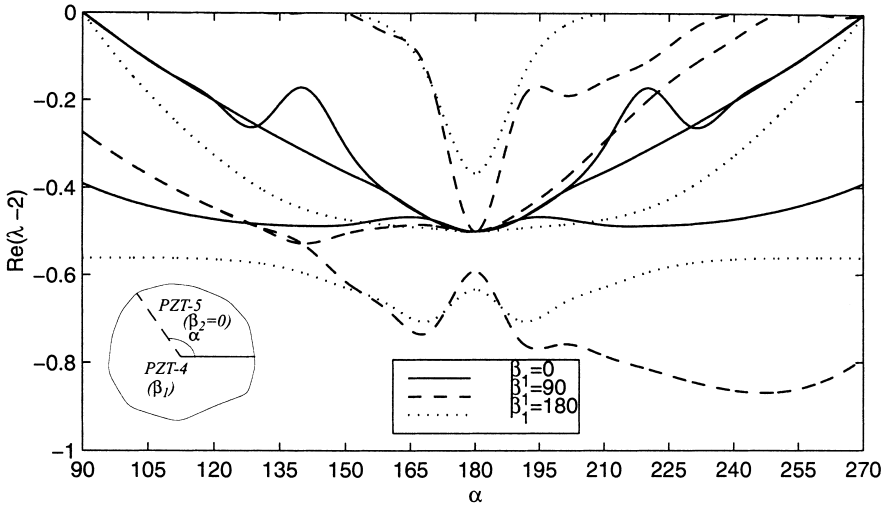

Fig. 10. Order of singularity for PZT-4–PZT-5 junctions with debonded interface.

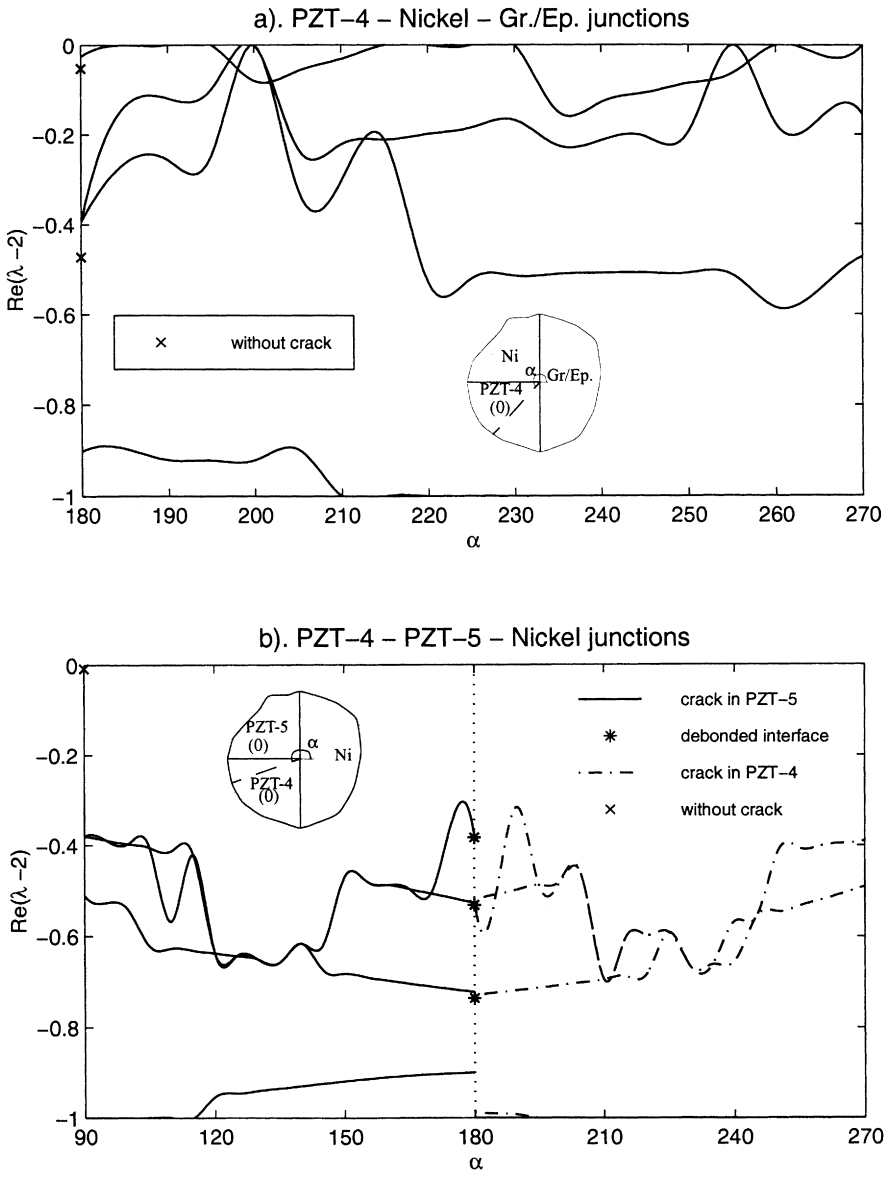

Fig. 11. Order of singularity for three material systems with a crack in piezoelectrics.

interface. The influence of α on the singularities is investigated for three different polarization orientations (β_1) of PZT-4 and for $\beta_2 = 0^\circ$. Three modes of singularities are generally observed and the significance of poling direction β_1 is clearly noted. The singularities are stronger than any of the previously considered cases. It is also interesting to note that roots for $\beta_1 = 0^\circ$ are not identical for $\beta_1 = 180^\circ$. The strongest singularity is noted when the two materials are polarized perpendicular to each other and α is greater than 180°. The singularity is relatively weaker when the two materials are polarized in the same direction when compared to opposite directions. Furthermore, the singularities are symmetrical about $\alpha = 180^\circ$ when the materials are polarized in the same or opposite directions. The

present case can be considered as a general case of a horizontal bi-material crack considered by Kuo and Barnett (1991. It is seen from Fig. 10 that for a horizontal interface crack ($\alpha = 180^\circ$), the strongest singularity is obtained when the two piezoelectric materials are polarized in opposite directions. Therefore the polarization orientations of both materials have a significant influence on the singular field near the tip of an interface crack between two piezoelectric materials. Other admissible homogeneous boundary conditions can be considered on the debonded interface and the results are not presented here for brevity.

5.5. Three material systems

Finally, the singularities in three dissimilar material systems, namely PZT, nickel and Gr./Ep. composite, are considered. Such material systems are encountered in adaptive structures, stack actuators, etc. The results are presented in Fig. 11 for two systems involving three materials. The direction of polarization is assumed to be along the z-axis. The system shown in Fig. 11(a) has a fully bonded interface between nickel and graphite/epoxy. Nickel–PZT and PZT–graphite/epoxy interfaces are both fully mechanically bonded, and electrically closed and insulated respectively. A crack is assumed in PZT-4 along the plane measured by the angle α. The crack faces have traction free and electrically open boundary conditions. The numerical results show two to four roots depending on the angle α. The singularities are very strong. The singularities corresponding this system in the absence of a crack is also shown in Fig. 11(a). Note the singularities become severe due to the presence of the crack. Fig. 11(b) shows results for a similar system involving PZT-4, PZT-5 and nickel. The crack is assumed to exist in one of the piezoelectric materials and $\alpha = 180^\circ$ corresponds to a debonded interface between PZT-4 and PZT-5. Three roots are found for the debonded PZT-4/PZT-5 interface case. One to four roots exist when the crack is inside the piezoelectric medium depending on the angle α. Note the singularities are discontinuous across the interface of PZT-4 and PZT-5. Again, the singularities are very strong. In the case of fully bonded junction without a crack, the singularity is very weak (-0.0078), as shown in the Fig. 11(b).

6. Conclusions

A general method of obtaining electroelastic singularities in piezoelectric wedges and composite piezoelectric wedges/junctions is successfully developed by extending Lekhnitskii's formalism for elastic anisotropic solids. The formulation is valid for an arbitrary polarization orientation. The characteristic equation governing the order of singularity is transcendental and the Müller's numerical method (1956) can be used to determine the roots accurately.

Compared to the corresponding elastic cases, piezoelectric wedges generally have one or more extra admissible roots. Electric boundary conditions show a significant effect on the order of singularities. The singularities of piezoelectric half planes and semi-infinite cracks are found to be invariant with respect to the directions of polarization. The polarization orientation has a negligible influence on singularities of piezoelectric wedges with identical boundary conditions on both surfaces. However for different boundary conditions on the edges, the order of singularities show strong dependence on the polarization angle.

The singularities are weaker for PZT–aluminum systems when compared to PZT–nickel systems. The strongest singularities of PZT–graphite/epoxy systems are -0.5, which correspond to the case of horizontal bi-material crack. Fully bonded PZT-graphite/epoxy junctions do not show any singularities. Bi-material systems of two piezoelectrics have stronger singularities that also depend significantly on the polarization direction. Two piezoelectrics polarized in the same or opposite directions show weaker

singularities when compared to bi-material systems with polarizations perpendicular to each other. Three material systems with a crack inside a piezoelectric medium have singularities stronger than the classical inverse square root singularity. The presence of a crack or a debonded interface result in a more severe singularity for both two and three material systems. The results presented in this study are useful in material selection, optimum design and failure analysis of adaptive structures and piezoelectric actuators. The present results are also useful to the development of special finite and boundary elements for accurate simulation of electroelastic fields at crack tips and sharp corners.

Acknowledgements

The work presented in this paper was supported by the Natural Sciences and Engineering Research Council of Canada grant A-6507. The authors thank a reviewer for bringing the paper by Chen and Lai (1997) to their attention.

Appendix

The constitutive equations for a piezoelectric medium in the Cartesian system (x', y', z') can be written as (Berlincourt et al., 1964)

$$[\epsilon'] = [s'][\sigma'] + [g']^{\mathrm{T}}[D'] \tag{A1}$$

$$[E'] = -[g'][\sigma'] + [\beta'][D'] \tag{A2}$$

For piezoelectrics with hexagonally symmetry with respect to z'-axis or piezoceramics polarized in the z'-direction, $[s']$, $[g']$ and $[\beta']$ are

$$[s'] = \begin{bmatrix} s'_{11} & s'_{12} & s'_{13} & 0 & 0 & 0 \\ s'_{12} & s'_{11} & s'_{13} & 0 & 0 & 0 \\ s'_{13} & s'_{13} & s'_{33} & 0 & 0 & 0 \\ 0 & 0 & 0 & s'_{44} & 0 & 0 \\ 0 & 0 & 0 & 0 & s'_{44} & 0 \\ 0 & 0 & 0 & 0 & 0 & 2(s'_{11} - s'_{12}) \end{bmatrix} \tag{A3}$$

$$[g'] = \begin{bmatrix} 0 & 0 & 0 & 0 & g'_{15} & 0 \\ 0 & 0 & 0 & g'_{15} & 0 & 0 \\ g'_{31} & g'_{31} & g'_{33} & 0 & 0 & 0 \end{bmatrix} \tag{A4}$$

$$[\beta'] = \begin{bmatrix} \beta'_{11} & 0 & 0 \\ 0 & \beta'_{11} & 0 \\ 0 & 0 & \beta'_{33} \end{bmatrix} \tag{A5}$$

where s'_{ij}, g'_{ij} and β'_{ij} denote elastic constants, piezoelectric constants and dielectric constants, respectively.

The constitutive equations in the Cartesian system (x, y, z) can be written in a form identical to Eq. (A1) and (A2). The coefficient matrices $[s]$, $[g]$ and $[\beta]$ in the (x, y, z) frame can be expressed in terms of

$$[s] = [h]^{\mathrm{T}}[s'][h]; \quad [g] = [a]^{\mathrm{T}}[g'][h]; \quad [\beta] = [a]^{\mathrm{T}}[\beta'][a] \tag{A6}$$

where angle β is shown in Fig. 2, and

$$[h] = \begin{bmatrix} \cos^2\beta & 0 & \sin^2\beta & 0 & -2\sin\beta\cos\beta & 0 \\ 0 & 1 & 0 & 0 & 0 & 0 \\ \sin^2\beta & 0 & \cos^2\beta & 0 & 2\sin\beta\cos\beta & 0 \\ 0 & 0 & 0 & \cos\beta & 0 & \sin\beta \\ \sin\beta\cos\beta & 0 & -\sin\beta\cos\beta & 0 & \cos^2\beta - \sin^2\beta & 0 \\ 0 & 0 & 0 & -\sin\beta & 0 & \cos\beta \end{bmatrix} \tag{A7}$$

$$[a] = \begin{bmatrix} \cos\beta & 0 & -\sin\beta \\ 0 & 1 & 0 \\ \sin\beta & 0 & \cos\beta \end{bmatrix}. \tag{A8}$$

For plane problems, the constitutive equations can be further simplified by applying the conditions of plain stress/strain. In the case of plain strain ($\epsilon'_{yy} = \epsilon'_{zy} = \epsilon'_{xy} = E'_y = 0$), Eq. (1) can be expressed in terms of s_{ij}, g_{ij}, β_{ij} as

$$a_{11} = s_{11} - s_{12}^2/s_{22}, \quad a_{12} = s_{13} - s_{12}s_{23}/s_{22}, \quad a_{13} = s_{15} - s_{12}s_{25}/s_{22}$$

$$a_{22} = s_{33} - s_{23}^2/s_{22}, \quad a_{23} = s_{35} - s_{23}s_{25}/s_{22}, \quad a_{33} = s_{55} - s_{25}^2/s_{22}$$

$$b_{11} = g_{11} - s_{12}g_{12}/s_{22}, \quad b_{21} = g_{31} - s_{12}g_{32}/s_{22}, \quad b_{12} = g_{13} - s_{23}g_{12}/s_{22}$$

$$b_{22} = g_{33} - s_{23}g_{32}/s_{22}, \quad b_{13} = g_{15} - s_{25}g_{12}/s_{22}, \quad b_{23} = g_{35} - s_{25}g_{32}/s_{22}$$

$$d_{11} = \beta_{11} + g_{12}^2/s_{22}, \quad d_{12} = \beta_{13} + g_{12}g_{32}/s_{22}, \quad d_{22} = \beta_{33} + g_{32}^2/s_{22}.$$

The constants $\mu'_n (n = 1, \ldots, 4)$ appearing in the Eq. (9) are the roots of the following equation

$$a_{11}\mu'^4 - 2a_{13}\mu'^3 + (2a_{12} + a_{33})\mu'^2 - 2a_{23}\mu' + a_{22} = 0 \tag{A9}$$

and

$$H'_{1n} = p'_n \cos\theta + q'_n \sin\theta; \quad H'_{2n} = -p'_n \sin\theta + q'_n \cos\theta \tag{A10}$$

where

$$p'_n = a_{11}\mu_n'^2 + a_{12} - a_{13}\mu'_n; \quad q'_n = (a_{12}\mu_n'^2 + a_{22} - a_{23}\mu'_n)/\mu'_n.$$

References

Berlincourt, D.A., Curran, D.R., Jaffe, H., 1964. Piezoelectric and piezoceramic materials and their function in transducers. In: Mason, W.P. (Ed.), Physical Acoustics, vol. I-A. Academic Press, New York.

Bogy, D.B., 1968. Edge-bonded dissimilar orthogonal elastic wedge under normal and shear loading. Transactions of the ASME, Journal of Applied Mechanics 35, 460–466.

Bogy, D.B., 1970. On the problem of edge-bonded elastic quarter-plane loaded at the boundary. International Journal of Solids and Structures 6, 1287–1313.

Chen, T., Lai, D., 1997. An exact correspondence between plane piezoelectricity and generalized plane strain in elasticity. Proceeding of the Royal Society, London Series A 453, 2689–2713.

Cheston, W.B., 1964. Elementary Theory of Electric and Magnetic Fields. Wiley.

Delale, F., 1984. Stress singularities in bonded anisotropic materials. International Journal of Solids and Structures 20, 31–40.

Dempsey, J.P., Sinclair, G.B., 1979. On the stress singular behaviour at the vertex of a bi-material wedge. Journal of Elasticity 9, 373–391.

Hein, V.L., Erdogan, F., 1971. Stress singularities in a two-material wedge. International Journal of Fracture 7, 317–330.

Kuo, C.M., Barnett, D.M., 1991. Stress singularities of interfacial cracks in bonded piezoelectric half-spaces. In: Wu, J.J., Ting, T.C.T., Barnett, D.M. (Eds.), Modern Theory of Anisotropic Elasticity and Applications. SIAM, Philadelphia, pp. 33–50.

Lekhnitskii, S.G., 1963. Theory of Elasticity of an Anisotropic Elastic Body. Holden-Day, New York.

Mantič, V., París, F., Cañas, J., 1997. Stress singularities in 2D orthotropic corners. International Journal of Fracture 83, 67–90.

Müller, D.E., 1956. A method for solving algebraic equations using an automatic computer. Mathematical Tables and Aids to Computation 10, 208–215.

Parton, V.Z., Kudryavtsev, B.A., 1988. Electromagnetoelasticity. Gordon and Breach Science Publishers, New York.

Sosa, H.A., Pak, Y.E., 1990. Three-dimensional eigenfunction analysis of a crack in a piezoelectric material. International Journal of Solids and Structures 26, 1–15.

Stroh, A.N., 1962. Steady state problems in anisotropic elasticity. Journal of Mathematics and Physics 41, 77–103.

Suo, Z., 1990. Singularities, interfaces and cracks in dissimilar anisotropic media. Proceeding of the Royal Society, London Series A 427, 331–358.

Ting, T.C.T., 1986. Explicit solution and invariance of the singularities at an interface crack in anisotropic composites. International Journal of Solids and Structures 22, 965–983.

Williams, M.L., 1952. Stress singularities resulting from various boundary conditions in angular corners of plates in extension. Transactions of the ASME, Journal of Applied Mechanics 19, 526–528.

Williams, M.L., 1956. The complex-variable approach to stress singularities-II. Transactions of the ASME, Journal of Applied Mechanics 23, 477–478.